Title

Subtitle

by

Mikkel Metzsch Jensen

THESIS

for the degree of

MASTER OF SCIENCE

Faculty of Mathematics and Natural Sciences
University of Oslo

Spring 2023

Title

Subtitle

Mikkel Metzsch Jensen

Title

http://www.duo.uio.no/

Printed: Reprosentralen, University of Oslo

Abstract

Abstract.

Acknowledgments

Acknowledgments.

Contents

List of symbols?

Maybe add list of symbols and where they are used like Trømborg.

Chapter 1

Background Theory and Method

1.1 Tribology - friction

Friction is a part of the wider field tribology which includes the study of friction, wear and lubrication between two surfaces in relative motion [1, p. 1]. In this thesis we will only concern ourselves with so-called wearless dry friction. That is, without any use of lubrication and without any resulting wear of the contacting surfaces. Tribological systems take place across a broad range of time and length scales, ranging from geological stratum layers involved in earthquakes [2] to microscopic atomistic processes, as in the gliding motion of a nanocluster of a nanomotor [3]. This vast difference in scale gives rises to different frictional mechanism being dominating at different scales. On a macro scale the system is usally subject to relatively high loads and speeds leading to high contact stresses and wear. On the other hand, the micro-/nanoscale regime occupies the opposite domain operating under relatviely small loads and speeds with negligible wear [2] [4, p. 5]. While macroscale friction is often reduced into a few variables such as load, material type, speed and surface roughness it is clear that the micro-/nanoscale friction cannot be generalized under such a simple representation. On the micro-/nanoscale the tribological propteries dominated by surface properties which will introduce an additional sensitivity variables such as temperature, humidity and even sliding history. The works of Bhushan and Kulkarni [5, (1996)] showed that the friction coefficient decreased with scale even though the materials used was unchanged. This reveals an intrinsic relationship between friction and scale as the contact condition is altered.

The phenomenological descriptions of macroscale friction cannot yet be derived from the fundamental atomic principles, and bridging the gap between different length scales in tribological systems remains an open challenge [3]. Hence, the following sections will be organized into macro-, micro- and nanoscale representing the theoretical understanding governing each scale regime. While our study of the graphene sheet is based on a nanoscale perspective the hypothesizing about application possibilities will eventually draw upon a macroscale perspective as well. Thus, we argue that a brief theoretical introduction to all three major scales is of high interest for a more complete interpreation of the findings in this thesis.

1.1.1 Macroscale

Our working definition of the *macroscale* is everything on the scale of visible everyday objects, which is usually denoted to the size of milimeters 10^{-3} m and above. Most importantly, we want to make a distinction to the microscale, where the prefix indicates the size of micrometers m^{-6}, and hence we essentially assign everything larger than *micro* to the term macroscale[1].

1.1.1.1 Amontons' law

In order to start and keep a solid block moving against a solid surface we must overcome certain frictional forces F_{fric} [1]. The static friction force F_s corresponds to the minimum tangential force required to initiate the sliding while the kintec friciton force F_k corresponds to the tangential force needed to sustain such sliding at steady speed. The work of Leonardo da Vinci (1452–1519), Guillaume Amontons (1663-705) and Charles de Coulomb

[1] The width of a human hair is on the length scale 10^{-5} to 10^{-4} m which constitute a reasonable boundary between macro- and microscale which fit well with a lower bound of human perception capabilities.

(1736-1806) all contributed to the empirical law, commonly known as Amontons' law, which serves as a common base for macroscale friction. Amontons' law states that the fricitonal forces is entirely independent of contact area and sliding velocity. Instead, it relies only on the normal force F_N, acting perpendicular to the surface, and the material specific friction coefficient μ as

$$F_{\text{fric}} = \mu F_N. \tag{1.1}$$

Notice that the term *Normal force* is often used interchangeably with *load* and *normal load* allthough the latter terms refer to the applied force, pushing the object into the surface, while the first is the corresponding reaction force acting from the surface on the object. These forces are exactly equal in magnitude and hence we will not make a clear distinction in this thesis. On the same note, the frictional force is different from a conventional force which in the Newtonian definition acts on a body from the outside and make it accelerate [6]. Rather than being an independent external force the friction force is an internal *reaction* force opposing the externally applied "sliding" force.

The friction coeffcient μ is typically different for the cases of static (μ_s) and kinetic (μ_k) friction, usually both with values lower than one and $\mu_s \geq \mu_k$ in all cases [1, p. 6]. The friction coefficient is taken to be a constant defined by either [6]

$$\mu = \frac{F_{\text{fric}}}{F_N}, \tag{1.2a}$$

or

$$\mu = \frac{dF_{\text{fric}}}{dF_N}. \tag{1.2b}$$

The first definition (1.2a) requires zero friction at zero load, i.e. $F_{\text{fric}} = 0 at F_N = 0$, while the second definition (1.2b) allows for a finite friction force at zero load since the coefficient is instead given by the slope of the F_{fric} versus F_N curve. However, in reality the friction coeffcient is not truly a material specific constant as it is often found to vary under different conditions such as humidity or smooth and rough morphologies of the sliding surfaces [6].

Although Amontons' law has been successful in is description of the majority of rubbing surfaces, involving both dry and lubricated, ductile and brittle and rough and smooth (as long as they are not adhesive) surfaces [6], it has its limitations. It is now known that eq. (1.1) is not valid over a large range of loads and sliding velocities and that it completely breaks down for atomically smooth surfaces in strongly adhesive contact [6]. The independency of sliding velocity dissapears at low velocities as thermal effects becomes important and for high velocities due to intertial effetcs [1, pp. 5-6]. For the case of static friction, it was later discovered to be dependent on the so-called contact history with increasing friction as the logarithm of time of stationary contact.

In cases where amontons' law breaks down we might still use the conceptual definition of the friction coefficient as defined by (1.2b). Especially, in the context of achieving negative friction coefficients (in certain load ranges) we would refer to this definition, since (1.2a) would imply a truly unphysical situation of the frictional force acting in the same direction as the sliding motion which would accelerate the object indefinitelly[2].

Due to the emperical foundation of Amontons' law it does not provide any physical insight into the underlying mechanisms of friction. However, as we will later discuss in more detail, we can understand the overall phenomena of friction through statistical mechanics by the concept of *equipartition of energy* [3]. A system in equilibrium has its kinetic energy uniformly distributed among all its degrees of freedom. When a macroscale object is sliding in a given direction it is clearly not in equilibrium since one of its degrees of freedom carriers considerable more kinetic energy. Thus, the system will have a tendency to transfer that kinetic energy to the remaining degrees of freedom as heat. This heat will dissipate to the sourroundings and the object will slow down as a result. Hence, we can understand friction simply the tendency of going toward equilibrium energy equipartitioning among many interacting degrees of freedom [3]. From this point of view it is clear that friction is an inevitable part of contact physics, but even though friction cannot be removed alltogether, we are still capable of manipulating it in usefull ways.

The attentive reader might point out that we have already moved the discussion partly into the microscopic regime as *statistical mechanics* generally aim to explain macroscale behaviour by microscopic interactions. In fact, this highlight the nessecity to consider smaller scales in order to achieve a more fundamental understadning of friction.

[2] You would most likely have a good shot at the Nobel Prize with that paper.

1.1.2 Microscopic scale

Going from a macro- to microscale perspective, a length scale of order 10^{-6} m, it was realized that most surfaces is in fact rough [7]. The contact between two surfaces consist of numerous smaller contact point, so-called asperities, for which the friction between two opposing surfaces involves interlocking of those asperities as visualized in figure 1.1. Small junctions of asperities are formed due to contact pressure and adhesion [2]

In the macroscale perspective of Amonton's law we refer to time- and space-averaged values, i.e. the "apparent" contact area and the average sliding speed [6]. However, microspocially we find the real contact area to be smaller than the macroscale apparent area and the shearing of local microjunctions can happen at large fluctuations or in a stick-slip fashion.

It is generally accepted that friction is caused by two mechanism: mechanical friction and chemical friction [2]. The mechanical friction is the "plowing" of the surface by hard particles or said asperities with an energy loss attributed to deformations of the asperity. While plastic deformations, corresponding to wear, gives rise to an obvious attribution for the energy loss, elastic deformations is also sufficient in explaining energy loss due to phonon excitations. In fact the assumption of plastic deformations has been critizised as this is theorized only to be present in the beginning of surface contact [8]. When machine parts slide against each other for millions of cycle the plastic deformation would only take place in the beginning until the system reaches a steady state with only elastic deformation taking place. The chemical friction arrises from adhesion between microscopic contacting surfaces, with an energy loss attributed to breaking and forming of bonds.

1.1.2.1 Surface roughness - Asperity theories

Asperity theories are based on the observation that microscopic rough surfaces, with contacting asperities each with a contact area of A_{asp}, will have a true contact area $\sum A_{\text{asp}}$ much smaller than the apperent macroscopic area [2]. The friction force has been shown to be proportional to the true contact area as

$$F_{\text{fric}} = \tau \sum A_{\text{asp}},$$

where τ is an effective shear strength of the contacting bodies. Note that this is compatible with Amontons' law in eq. (1.1) by having a linear relatioship between the real contact area and the applied load. In figure 1.1 we see a visualization on how the contact area might intuitively increase with load as the asperity tips is deformed (plastically or elastically) into broader contact points.

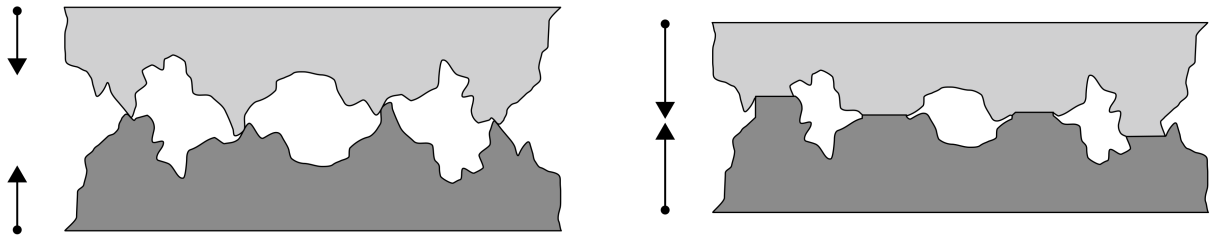

(a) Low load. **(b)** High load.

Figure 1.1: Qualitatively illustration of the microscopic asperity deformation under increasing load from frame (a) to (b) [9]. While this figure evidently portrays plastic deformation the concept of increased contact area under increased load applies for elastic deformation as well.

Many studies have focused on single asperity contacts to reveal the relationship between the contact area and F_N (13-15 from [7]). By assuming perfectly smooth asperities, with radii of curvature from micrometers all the way down to nanometers, continuum mechanics can be used to predict the deformation of asperities as load is applied. A model for non-adhesive contact between homogenous, isotropic, linear elastic spheres was first developed by Hertz (17 from [7]), which predicted $A_{\text{asp}} \propto F_N^{2/3}$. Later adhesion effects were included in a number of subsequent models, including Maugis-Dugdale theory (18 from [7]), which also predicts a sublinear relatinship between A_{asp} and F_N. Thus, the common feature of all single-asperity theories is that A_{asp} is a sublinear function of F_N, leading to a similar sublinear relationship for $F_{\text{fric}}(F_N)$, which fails to align with the macroscale observations modelled by Amontons' law (eq. (1.1)).

Concurrently wiht single-asperity studies, roughness contact theories are being developed [7, 8-10, 16 in] to bridge the gap between single asperities and macroscopic contacts [7]. A variety of multi-asperity theories has attempted to combine single asperity mechanics by statistical modelling of the asperity height and spatial distributions [8]. This has led to a partially success in the establishment of a linear relationship between A_{asp} and F_N. Unfortunately, these results are restricted in terms of the magnitude of the load and contact area, where multi-asperity contact models based on the original ideas of Greenwood and Williamson [10] only predicts linearity at vanhising low loads, or Persson [11] which works for more reasonable loads but only up to 10-15 % of the macroscale contact area. However, as the load is furhter increased all multi-asperity models predict the contact area to fall into the sublinear dependency of normal force as seen for single aperity theories as well [8].

1.1.3 Nanoscale - Atomic scale

Going from a micro- to a nanoscale, on the order of 10^{-9} m, it has been predicted that continnum mechanics will break down [12] due to the discreteness of individual atoms. Note that atom spacing lies in the domain of a few ångströms Å (10^{-10} m) and thus we take the so-called atomic-scale to be a part of the nanoscale regime. In a numerical study by Mo et al. [7] (considering asperity radii of 5-30 nm) it has been shown that the asperity area A_{asp}, defined by the circumfereance of the contact zone, is sublinear with F_N. This is accommodated by the observation that not all atoms within the circumfereance make chemical contact with the substrate. By modelling the real contact area $A_{\text{real}} = NA_{\text{atom}}$, where N is the amount of atoms within the range of chemical interaction and A_{atom} the associated surface area for an atom, they found a consistent linear relationship between friction and the real contact area. Without adhesive forces this lead to a similar linear relationship $F_{\text{fric}} \propto F_N$, while adding van der Waals adhesion to the simulation gave a sublinear relatinship, even though the $F_{\text{fric}} \propto A_{\text{real}}$ was maintained. This result emphasizes that the contact area is still expected to be play an important role at the nanoscale for asperity theory. It is simply the definition of the contact area that undergoes a change when transistioning from micro- to nanoscale.

However, considering the simulation setup of our numerical study, a flat sheet on a flat substrate, the lack of asperities make it unfounded to rely on asperity theories. Although both numerical and experimental research have been done for so-called nanoflakes sliding on a substrate, no investigation is reported on the dependence of friction force on contact area (to the best of my knowledge at least). One reasonable explanation is that the contact area is already maxed out for atomic smooth surfaces. Since a dependency on normal load is still reported in most nanoflake studies (see section 1.1.3.3 or give details on studies here?), this suggests that some other mechanisms are governing friction at this level. Before diving into alternative theoretical approaches to adress this issue we point out that exactly this transistion, between nanoscale asperities and atomic smooth surfaces, is of outermost importance for the objective of the thesis. By introducing kirigami cuts and stretching the sheet we expect to see an out of plane buckling which induce an ensemble of asperities on the sheet. Hence, we might hypothesize that such a transsition will contribute to a significant change in the goverening mechanism of friction bridgering two (poorly understood) theoretical domains

In the lack of noteworthy structural asperities, friction can instead be modelled as a consequencse of the rough potential of the atomic landscape. A series of models builds on this idea by considering different ways for the atoms to interact interatomically, with the moving body, and the substrate. In figure 1.2 three of the most common 1D models is displayed. The time-honered Prandtl-Tomlinson (PT) model describes a point-like tip sliding over a space-periodic fixed crystalline surface with a harmonic coupling to the *moving body*. This is analog to that of an experimental cantilever used for Atomic Force Microscopy (see section 1.1.3.2). Further extensions was added in the Frenkel-Kontorova (FK) model by substituting the tip with a chain of harmonic coupled atoms dragged from the end (I am not sure that the figure is 100% correct by drawing a spring like that), and finally combinned in the Frenkel-Kontorova-Tomlinson (FKT) with the addition of a harmonic coupling between the chain and the moving body. In the following we will disucss the FK model as this gives provides a sufficient foundation for the understanding of smooth nanoscale friction.

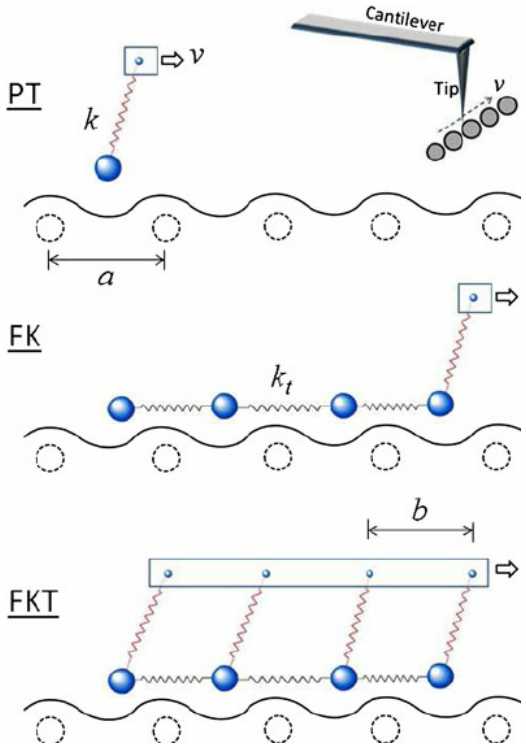

Figure 1.2: Temporary figure from https://www.researchgate.net/figure/Illustrations-of-the-1D-PT-FK-and-FKT-models-Large fig1_257670317

1.1.3.1 Frenkel-Kontorova

The standard Frenkel-Kontorova (FK) model consists of a 1D chain of N classical particles of equal mass, representing atoms, interacting via hamornic forces and moving in a sinusoidal potential as sketched in figure 1.3 [3]. The hamiltonian is

$$H = \sum_{i=1}^{N} \left[\frac{p_i^2}{2m} + \frac{1}{2}K(x_{i+1} - x_i - a_c)^2 + \frac{1}{2}U_0 \cos\left(\frac{2\pi x_i}{a_b}\right) \right], \tag{1.3}$$

where the atoms are labelled sequently $i = 1, \ldots, N$. The first term $p_i^2/2m$ represents the kinetic energy with momentum p_i and mass m. Often the effetcs of inertia are neglected, reffered to as the static FK model, while the inclusion, as shown here in eq. (1.3), is known as the dynamic FK model [13]. The next term describes the harmonic interaction with elastic constant K, nearest neighbour distance $\Delta x = x_{i+1} - x_i$ and corresponding nearest neighbour equilibrium distance a_c. The final term represents the periodic substrate potential (external potential on site) with amplitude U_0 and period a_b. Different boundary choices can be made where both free ends and periodic conditions gives similar results. The choice of fixed ends however makes the chain incapable of sliding.

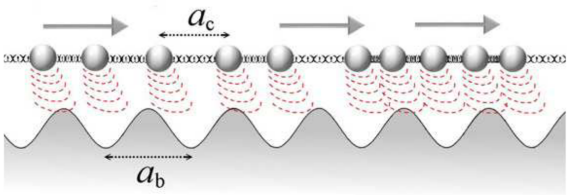

Figure 1. A sketch of the FK model, showing the two competing lengths: the average interparticle spacing and the lattice periodicity of the substrate.

Figure 1.3: Temporary figure from [3]

To probe static friction one can apply an external adiabatically increasing force until sliding accours. This corresponds to the static FK model, and it turns out that the sliding properties are entirely governed by its topological excitations referred to as so-called *kinks* and *antikinks*

Commensurability We can subdivide the frictional behaviour in terms of commensurability, that is, how well the spacing of the atoms match the periodic substrate potential. We describe this by the length ratio $\theta = a_b/a_c = N/M$ where M denotes the number of minemas in the potential (within the length of the chain). A rational number for θ means that we can align the atoms in the chain perfectly with the minemas, without stretching the chain, corresponding to a *commensurate* case. If θ is irrational the chain and substrate cannot fully align without stretching of the chain, and we denote this as being *incommensurate*.

We begin with the simplest commensurate case of $\theta = 1$ where the spacing of the atoms matches perfectly with the substrate potential periodicity, i.e. $a_c = a_b$, $N = M$. The ground state (GS) is the configuration where each atom fits in one of the substrate minema. By adding an extra atom we would effectively shift over some atoms, away from this ideal state, giving rise to a kink excitation, i.e. two atoms will have to "share" the same potential corrugation as sketched in figure 1.5. On the other hand, removing an atom from the chain results in an antikink excitation where one potential corrugation will be left "atomless". In order to reach a local minimum the kink (antikink) will expand in space over a finite length such that the chain undertakes a local compression (expansion). When applying a tangential force to the chain it is much easier for an excitation to move along the chain than it is for the non-exicted atoms since the activation energy ϵ_{PN} for a kink/antikink displacement is systematically smaller (often much smaller) than the potential barrier U_0. Thus, the motion of kinks (antikinks), i.e. the displacement of extra atoms (atom vacancies), is represententing the fundamental mechanism for mass transport. These displacements are responsible for the mobility, diffusivity and conductivity within this model.

In the ideal zero temperature commensurable case with an adiabatical increase in force, all atoms would be put into an accelerating motion as soon as the potential barrier energy is present ($\sim NU_0$ for sufficiently stiff springs). However, in reality any thermal excitation would excite the system before this point is reached resulting in kink-antikink pairs traveling down the chain. For a chain of finite length these often accour at the end of the chain running in opposite direction. As a kink travels down the chain the atoms is advanced by one lattice spacing a_b along the substrate potential. This cascade of kink-antikink exications is shown in figure 1.4

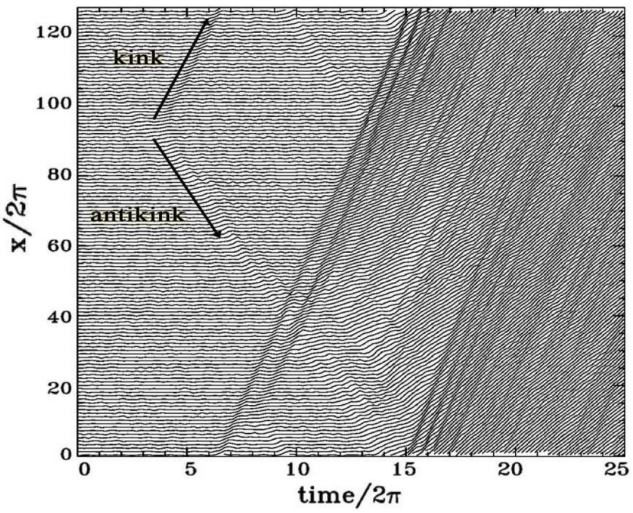

Figure 2. Time dependence of the atomic trajectories for the fully matched ($\theta = 1$) FK model at the (low-temperature) onset of depinning. Motion starts with the nucleation of a kink-antikink pair. The kink and the antikink depart in opposite directions cross the periodic boundary conditions, and collide quasielastically. A second kink-antikink pair forms in the wake of the initial kink. Further kink-antikink pairs are generated, with an avalanche-like increase of the kink-antikink concentration, eventually leading to a sliding state. Adapted from Ref. [21], Copyright (1997) by The American Physical Society.

Figure 1.4: Temporary figure from [3]

For the 2D case where an island (or flake) is deposited on a surface, in our case the graphene sheet on the Si substrate, we generally also expect the sliding to be initated by kink-antikink pairs at the boundary.

For the case of incommensurability, i.e. $\theta = a_b/a_c$ is irrational, the GS is characterized by a sort of ´´staircase" deformation. That is, the chain will exhibit regular periods of regions where the chain is slightly compressed (expanded) to match the substrate potential, seperated by kinks (antikinks), where the increased stress is eventually released through a localized expansion (compression) as illustrated in figure 1.5 Go through this last part again. Even though this is what the source says I'm not quite sure I understand why it is not opposite "...released through a localized compression (expansion)"?.

Figure 1.5: Temporary figure from urlhttp://www.iop.kiev.ua/ obraun/myreprints/surveyfk.pdf p. 14. Incommensurable case (θ =?) where atoms sits slightly closer than otherwise dictated by the substrate potential for which this regularly result in a kink here seen as the presence of two atoms closely together in on of the potential corrugations.

The incommensurable FK model contains a critical elastic constant K_c, such that for $K > K_c$ the static friction F_s drops to zero, making the chain able to initiate a slide at no energy cost, while the low-velocity kinetic friction is dramatically reduced. This can be explained by the fact that the displacement accouring in the incommensurable case will yield just as many atoms climbing up a corrugation as there are atoms climbing down. For a big (infinite) chain this will exactly balance the forces making it non-resistant to sliding. Generally, incommensurability guarantees that the total energy (at $T = 0$) is independent of the relative position to the potential. However, when sliding freely a single atom will eventually occupy a maximum of the potential. When increasing the potential magnitude U_0 or softning the chain stiffness, lowering K, the possibility to occupy such

a maximum dissapears. This marks the so-called Aubry transition at the critical elasric constant $K = K_c(U_0, \theta)$ where the chain goes from a free sliding to a *pinned state* with a nonzero static friction. K_c is a discontinuous function of the ratio θ, due to the reliance on irrational numbers for incommensurability. The minimal value $K_c \simeq 1.0291926$ in units $[2U_0(\pi/a_b)^2]$ is achieved for the golden-mean ratio $\theta = (1 + \sqrt{5}/2)$. Notice that the pinning is provided despite translational invariance due to the inaccessibility to move past the energy barrier which act as a dynamical constraint. The Aubry transistion can be invistigated as a first-order phase transistion for which power laws can be defined for the order parameter. This is beyond the scope of this thesis as we merely are going to point to the FK model for the understanding of stick-slip behvaiour and the concept of commensurability.

The phenonema of non-pinned configurations is named *superlubricity* in tribological context. Despite the misleadning name this referes to the case where the static friction is zero while the kinetic friction is nonzero but reduced. For the case of a 2D sheet it is possible to alter the commensurability by changing the orientation of the sheet relative to the substrate. This has been shown for a graphene flake sliding over a graphite surface (multiple layers of graphene) [14] as shown in figure 1.6. We clearly see that friction changes as a function of orientation angles with only two spikes of considerable friction force.

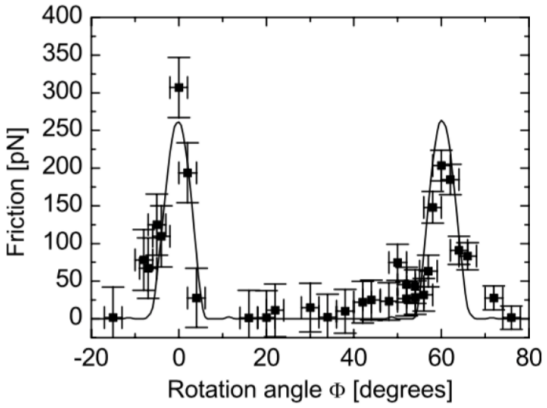

Fig. 6. Average friction force versus rotation angle Φ of the graphite sample around an axis normal to the sample surface. Two narrow peaks of high friction are observed at 0° and 61°, respectively. Between these peaks a wide angular range with ultra-low friction, close the detection limit of the instrument, is found. The first peak has a maximum friction force of 306 ± 40 pN, and the second peak has a maximum of 203 ± 20 pN. The curve through the data points shows results from a Tomlinson model for a symmetric 96-atom graphite flake sliding over the graphite surface (for details about the calculation see [39]).

Figure 1.6: Temporary figure from [14] showing superlubricity for incommensurable orientations between graphene and graphite. temporary

Kinetic friction In the FK model the kinetic friction is primarily caused by resonance between the sliding induced vibrations and phonon modes in the chain [13]. The specific dynamics is found to be highly model and dimension specific, and even for the 1D case this is rather complex. However, we make a simplified analysis of the 1D case to showcase the reasoning behind the phenomena.

When all atoms are sliding rigidly width center of mass velocity v_{CM} the atoms will pass the potential maxima with the so-called *washboard frequency* $\Omega = 2\pi v_{\mathrm{CM}}/a_b$. For a weak coupling between the chain and the potential we can use the zero potential case as an approximation for which the known dispersion relation for the 1D harmonic chain is given [Kittel (add to bibliography)]

$$\omega_k = \sqrt{\frac{4K}{m}} \left| \sin\left(\frac{k}{2}\right) \right|,$$

where ω_k is the phonon frequency and $k = 2\pi i/N$ the wavenumber with $i \in [N/2, N/2)$. Resonance will accour when the washboard frequency Ω is close to the frequency of the phonon modes ω_q in the chain with wavenumber $q = 2\pi a_c/a_b = 2\pi\theta^{-1}$ or its harmonics nq for $n = 1, 2, 3, \ldots$ [15]. Thus, we can approximate the resonance COM speed as

$$\begin{aligned} n\Omega &\sim \omega_{nq} \\ n\frac{2\pi v_{\mathrm{CM}}}{a_b} &\sim \sqrt{\frac{4K}{m}}\left|\sin\left(\frac{2n\pi\theta^{-1}}{2}\right)\right| \\ v_{\mathrm{CM}} &\sim \frac{\sin\left(n\pi\theta^{-1}\right)}{n\pi}\sqrt{\frac{Ka_b^2}{m}}. \end{aligned}$$

When the chain slides with a velocity around resonance speed, the washboard frequency can excite acoustic phonons which will dissipate to other phonon modes as well. At zero temperature the energy will transform back and forth between internal degrees of freedom and center of mass movement of the chain. Hence, at zero temperature this is in fact theorized to speed up the translational decay. However, for the more realistic case of a non-zero temperature the substrate serves as a thermostat, for which energy will dissipate from the chain to the substrate degrees of freedom, giving rise to kintetic friction. This suggets that certain sliding speeds will exhibit relatively big kinetic friction while others will be subject to extremely low kinetic friction. Simulations of concentric nanotubes in relative motion (telescopic sliding) have revealed the occurence of certain velocities at which the friction is enhanced, corresponding to the washboard frequency of the system [3]. The friction response was observed to be highly non-linear as the resonance velocities were approached.

A common way to model the non-zero temperature case is by the use of a Langevin thermostat, which models the dissipation of heat by adding a viscous damping force and thermal fluctuations by the addition of Gaussian random forces with variance proportional to the temperature (This is covered in more details in section **??**). In combination, this gives rise to a kinetic friction that is both velocity and temperature dependent.

By extending the FK model into 2D [13] it can be shown numerically that the friction coefficient generally increases with increasing velocity and temperature resepectively, although the specific of the trend is highly sensitive to model parameters.

Temperature depence Might find something interesting here [16] or [17].

Smooth sliding Find a suitable place to introduce smooth sliding. Above certain velocities the stick-slip motion dissapear. [1, p. 142-ish]

1.1.3.2 Experimental procedures

[1]

Experimentally nanoscale friction is challenging to approach as the forces, on the scale of nano-newtons as well, is extremely small. Additionally surface topography is not easily viewed. On the other side simulations provide full transparency regarding information of the physical structure of the sample among with forces, velocities and temperature. However, in order to compare numerical results the experimental procedures is most often mirrored in simulations. Thus it is beneficial to adress the most common experimental techniques when designing a simulation.

Scanning Probe Microscopy Scanning probe microscopy (SPM) includes a variety of experimental methods which is used to examine surfaces with atomic resolution [18, p. 6-]. This was orginally developed for surface topography imaging, but today it plays a crucial role in nanoscale science as it is used for probe-sampling regarding tribological, electronic, magnetic, biological and chemical character. The famility of methods involving the measurement of forces is generally referred to as *scanning force microscopies* (SFM).

One such method arose from the *atomic force micrpscope*, which consist of a sharp micro-fabricated tip attacthed to a contilever force sensor, usually with a sensitivy below 1 nN. The force is measured by recording the bending of the cantilever, either as a change in electrical conduction or more commonly, by a light beam reflected from the back of the cantilever into a photodetector [1]. By adjusting the tip-sample height to keep a constant normal force while scanning accross the surface this can be used to produce a surface topography map. By tapping the material (dynamic force microscopy) with sinusoidally vibrated tip the effects from friction

and other disturbing forces can be minimized in order to produce a clear image (include example, preferable of graphene). However, when scanning perpendicularly to the cantilever axis one is also able to measure the frictional force as torsion of the cantilever. By having four quadrants in the photodetector (as shown in figure 1.7), one can simultaneously measure the normal force and friction force as the probes scans accross the surface.

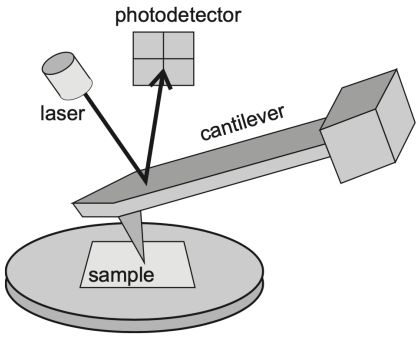

Figure 17.1 Schematic diagram of a beam-deflection atomic force microscope.

Figure 1.7: Temporary figure from [1, p. 184]

This can also be used to drag a nanoflake as done by Dienwiebel et al. [14] (earlier referrenced), where a graphene flake was attahced to a FFM tip and dragged accross graphite.

Surface Force Apparatus (SFA) Is this the one where to surfaces slides in opposite direction (at least that is the commen MD way I see it.)

1.1.3.3 (summary of) Expected frictional properties

The setup of our simulation is most reminiscent of a graphene flake sliding on a substrate. This has been studied numerically in molecular dynamic simulations by Zhu and Li [19, 2018] for a graphene flake on a gold substrate and by Zhang et al. [20](2019) on a diamond substrate, and in a tight-binding simulation by Bonelli et al. [21](2009) for graphene on graphite. Experimental studies of a graphene flake attatched to a AFM is done by Dienwiebel et al. [14, 2005] and Feng et al. [22, 2013] sliding on graphite, but these are mainly concerned with superlubricity as a function of flake oreientation commensurability.

In our study we simmulate a graphene flake on a silicon substrate which deviates slightly from the above-mentioned reference. Additionally, the normal force is only applied to the ends of the sheet. Obviously stretching and cutting the sheet will seperate our study dramatically from the references, but we aim to compare the frictional properties to the reference before applying stretch or cuts.

Qualitatively we have the following expectations for the unstretched and non-cut graphene sheet.

Qualitatively

1. Stick slip: Generally expect to see periodic stick-slip motion with a period mathing the lattice constant(s) involved [7]. This was both present in the MD simulations [19], [20] and in the experiment by [14]. In AFM and SFA experiemnts, the stick-slip motion tend to transistion into smooth sliding when the speed exceeds $\sim 1\mu$ m/s while in MD modelling the same transistion is observed in the $\sim 1m/s$ region [3]. This 6 order of magnitude discrepancy has been largely discussed in connection to simplifying assumptions in MD simulations.Bonelli et al. [21] found that the stick-slip behaviour was present when the cantilever-tip-flake coupling was done with a relatively soft springs in contrast to hard springs which inhibited it.

2. Static friction: As highlighted in the FK model static friction will be sensitive to commensurability, which will additionally be affected by flake size. Reguzzoni and Righi [23] have shown that the effective commensurability will increase drastically below a critical flake radius on the order of 10 Å. Macroscopically we expect to see a logarithmic increase in friction with time [24], and hence due to the short time-span of the static contact before dragging, it is not easy to estimate whether a significant static friction peak will be found.

3. Oritentation (friction anisotropy): As predicted by the FK model and confirmed both numerically [19], [20] and experimentally [14], [22] we expect to see a dependence of friction force on orientation due to changing commensurability. Zhu and Li [19] (gold substrate) reported the highest friction when sliding along the armchair direction, while Zhang et al. [20] (diamond substrate) found the zigzag-direction to give the highest friction force along the zigzag direction (also the most evident stick-slip behvaiour).

Table 1.1: Quantitative nano friction dependence on various variables.

Variable	Dependency	Numerical studies	Experimental
Normal force F_N	$F_{\text{fric}} \propto F_N^{\alpha}$ $\alpha \leq 1$	Zhang et al. [20] finds a seemingly linear relationship $F_{\text{fric}} \propto F_N$ while Bonelli et al. [21] reports a sublinear relationship. The latter corresponds with that of nanosasperity simulations where [7] (amorphous carbon tip and a diamond sample) also found sublinear relationship when including adhesion.	Experimentally different trends have been observed [1, p. 200]. For the graphebne flake Dienwiebel et al. [14] found a non-dependent relationship while Feng et al. [22] did report on this. FFM analog to the single asperity setup have yielded both linear relationship [6] (silicon tip on gold) while Schwarz et al. [25] found that FFM with well-defined spherical tips mathed with theoretical results(DMT, elastic spheres pressed together [1, p. 200]), yielding a power law $F_{\text{fric}} = F_N^{2/3}$.
Velocity v	$F_{\text{fric}} \propto \ln v$		Logaritmic velocity dependence of friction has been measured for nanotip friction [1, p. 201] associated to thermal activation and possibly the time availble to form bond between the tip and the substrate. At higher velocities thermally activated processes are less important and friction becomes independent of velocity. This has been observed for Si tips and diamond, graphite and amorphous carbon surfaces with scan velocities above 1 μm/s.
Temperature T	Either increase (MD) or decrease as $F_{\text{fric}} \propto \exp(1/T)$ (experimental)	Zhang et al. [20] found tha friction increased with temperature.	Zhao et al. [16] found $F_{\text{fric}} \propto \exp(1/T)$
Real contact area A	$F_{\text{fric}} \propto A$	Mo et al. [7] found that $F_{\text{fric}} \propto A$ where A is the real contact area defined by atoms within chemical range. This is not studied for the case of a nanoflake where the contact area is presumingly rather constant.	

Appendices

Appendix A

Bibliography

[1] E. Gnecco and E. Meyer, *Elements of Friction Theory and Nanotribology*. Cambridge University Press, 2015, 10.1017/CBO9780511795039.

[2] H.-J. Kim and D.-E. Kim, *Nano-scale friction: A review*, .

[3] N. Manini, O. M. Braun, E. Tosatti, R. Guerra and A. Vanossi, *Friction and nonlinear dynamics*, *Journal of Physics: Condensed Matter* **28** (jun, 2016) 293001.

[4] Bhusnan, *Introduction*, ch. 1, pp. 1–? John Wiley & Sons, Ltd, 2013. https://onlinelibrary.wiley.com/doi/pdf/10.1002/9781118403259.ch1. https://doi.org/10.1002/9781118403259.ch1.

[5] B. Bhushan and A. V. Kulkarni, *Effect of normal load on microscale friction measurements*, *Thin Solid Films* **278** (1996) 49–56.

[6] J. Gao, W. D. Luedtke, D. Gourdon, M. Ruths, J. N. Israelachvili and U. Landman, *Frictional forces and amontons' law: From the molecular to the macroscopic scale*, .

[7] Y. Mo, K. T. Turner and I. Szlufarska, *Friction laws at the nanoscale*, .

[8] G. Carbone and F. Bottiglione, *Asperity contact theories: Do they predict linearity between contact area and load?*, *Journal of the Mechanics and Physics of Solids* **56** (2008) 2555–2572.

[9] W. Commons, *File:asperities.svg — wikimedia commons, the free media repository*, 2022.

[10] J. A. Greenwood and J. B. P. Williamson, *Contact of nominally flat surfaces*, Dec, 1966. 10.1098/rspa.1966.0242.

[11] B. N. J. Persson, *Theory of rubber friction and contact mechanics*, *The Journal of Chemical Physics* **115** (2001) 3840–3861, [https://doi.org/10.1063/1.1388626].

[12] B. Luan and M. O. Robbins, *The breakdown of continuum models for mechanical contacts*, .

[13] J. Norell, A. Fasolino and A. Wijn, *Emergent friction in two-dimensional frenkel-kontorova models*, *Physical Review E* **94** (04, 2016) .

[14] M. Dienwiebel, N. Pradeep, G. S. Verhoeven, H. W. Zandbergen and J. W. Frenken, *Model experiments of superlubricity of graphite*, *Surface Science* **576** (2005) 197–211.

[15] J. A. van den Ende, A. S. de Wijn and A. Fasolino, *The effect of temperature and velocity on superlubricity*, *Journal of Physics: Condensed Matter* **24** (oct, 2012) 445009.

[16] X. Zhao, M. Hamilton, W. G. Sawyer and S. S. Perry, *Thermally activated friction*, .

[17] S. Y. Krylov, K. B. Jinesh, H. Valk, M. Dienwiebel and J. W. M. Frenken, *Thermally induced suppression of friction at the atomic scale*, *Phys. Rev. E* **71** (Jun, 2005) 065101.

[18] B. Bhushan, *Nanotribology and nanomechanics*, *Wear* **259** (2005) 1–?

[19] P. Zhu and R. Li, *Study of nanoscale friction behaviors of graphene on gold substrates using molecular dynamics*, .

[20] J. Zhang, E. Osloub, F. Siddiqui, W. Zhang, T. Ragab and C. Basaran, *Anisotropy of graphene nanoflake diamond interface frictional properties*, *Materials* **12** (2019) .

[21] F. Bonelli, N. Manini, E. Cadelano and L. Colombo, *Atomistic simulations of the sliding friction of graphene flakes*, .

[22] X. Feng, S. Kwon, J. Y. Park and M. Salmeron, *Superlubric sliding of graphene nanoflakes on graphene*, .

[23] M. Reguzzoni and M. C. Righi, *Size dependence of static friction between solid clusters and substrates*, *Phys. Rev. B* **85** (May, 2012) 201412.

[24] J. H. Dieterich, *Time-dependent friction in rocks*, *Journal of Geophysical Research (1896-1977)* **77** (1972) 3690–3697, [https://agupubs.onlinelibrary.wiley.com/doi/pdf/10.1029/JB077i020p03690].

[25] U. D. Schwarz, O. Zwörner, P. Köster and R. Wiesendanger, *Quantitative analysis of the frictional properties of solid materials at low loads. i. carbon compounds*, *Phys. Rev. B* **56** (Sep, 1997) 6987–6996.